# Discovery of a heme-binding domain in a neuronal voltage-gated potassium channel

Mark J. Burton, Joel Cresser-Brown, Morgan Thomas, Nicola Portolano, Jaswir Basran, Samuel L. Freeman, Hanna Kwon, Andrew R. Bottrill, Manuel J. Llansola-Portoles, Andrew A. Pascal, et al.

# A heme-binding domain in a neuronal voltage-gated potassium channel

Mark J Burton[‡,*], Joel Cresser-Brown[§,*], Morgan Thomas[‡], Nicola Portolano[‡], Jaswir Basran[¶], Samuel, L. Freeman[§], Hanna Kwon[§], Andrew R. Bottrill[†], Manuel J Llansola-Portoles[□], Andrew A. Pascal[□], Rebekah Jukes-Jones[§§], Tatyana Chernova[§§], Ralf Schmid[¶], Noel W Davies[¶], Nina M Storey[¶], Pierre Dorlet[||], Peter C E Moody[¶], John S Mitcheson[¶] and Emma L Raven[§,1]

[‡] Department of Chemistry and Leicester Institute of Structural and Chemical Biology, University of Leicester, Leicester, LE1 7RH, England.
[§] School of Chemistry, University of Bristol, Cantock's Close, Bristol, BS8 1TS, UK.
[¶] Department of Molecular and Cell Biology and Leicester Institute of Structural and Chemical Biology, University of Leicester, Leicester, LE1 9HN, England.
[†] Protein Nucleic Acid Chemistry Laboratory, Hodgkin Building, University of Leicester, LE1 9HN, UK.
[□] Université Paris-Saclay, CEA, CNRS, Institute for Integrative Biology of the Cell (I2BC), 91198, Gif-sur-Yvette, France.
[§§] MRC Toxicology Unit, University of Cambridge, Lancaster Rd, Leicester, LE1 9HN, UK.
[||] CNRS, Aix Marseille Univ, BIP, Marseille, France.
[1] To whom correspondence should be addressed. School of Chemistry, University of Bristol, Cantock's Close, Bristol, BS8 1TS, UK. Telephone: +44 (0)117 9287647; E-mail: emma.raven@bristol.ac.uk.

*Running title*: A heme-binding domain in hERG3.

*Keywords*: heme, hERG3, ion channel, PAS domain, Cap domain, heme regulation.

[1] To whom correspondence should be addressed. School of Chemistry, University of Bristol, Cantock's Close, Bristol, BS8 1TS, UK. Telephone: +44 (0)117 9287647; E-mail: emma.raven@bristol.ac.uk.

[*] These authors contributed equally to this work.

## ABSTRACT

The *ether-à-go-go* (EAG) family of voltage gated $K^+$ channels are important regulators of neuronal and cardiac action potential firing (excitability) and have major roles in human diseases such as epilepsy, schizophrenia, cancer and sudden cardiac death. A defining feature of EAG (Kv10-12) channels is a highly conserved domain on the amino-terminus, known as the eag-domain, consisting of a PAS domain capped by a short sequence containing an amphipathic helix (Cap-domain). The PAS and Cap domains are both vital for the normal function of EAG channels. Using heme-affinity pull-down assays and proteomics of lysates from primary cortical neurons, we identified that an EAG channel, hERG3 (Kv11.3), binds to heme. In whole cell electrophysiology experiments, we identified that heme inhibits hERG3 channel activity. In addition, we expressed the Cap and PAS domain of hERG3 in *E.coli* and, using spectroscopy and kinetics, identified the PAS domain as the location for heme binding. The results identify heme as a regulator of hERG3 channel activity. These observations are discussed in the context of the emerging role for heme as a regulator of ion channel activity in cells.

## INTRODUCTION

PAS (Per-ARNT-Sim) domains, first identified by sequence homology in the *Drosophila* proteins *period* and *single*-minded, and the vertebrate aryl hydrocarbon receptor nuclear transporter (ARNT), are well known sensory modules present in a variety of signalling proteins in organisms ranging from bacteria to humans (1-3). PAS domains demonstrate considerable plasticity in binding different biologically-relevant ligands. Relevant in the context of this work is their ability to bind heme as a ligand. The ligand binding event is significant as it can act as a primary trigger to initiate a cellular signalling / regulatory response; or, it can provide the PAS domain with a capacity to respond to secondary physical or chemical signals (such as binding of gas molecules, changes in redox potential, or light activation). In the case of heme as a ligand, there are several examples of heme-binding PAS domains that act as biological regulators in cells, for example the $O_2$ sensor proteins (*e.g.* FixL, *E. coli* DOS) and the transcriptional regulators involved in circadian control (*e.g.* nPAS2, CLOCK, Rev-ERB, Per) (4,5).

Several layers of regulatory control can be envisaged in the process of heme binding to a PAS domain protein. Heme binding might, for example, induce a conformational change in the PAS domain which affects the interactions with partner proteins, and there is evidence for this in the heme-binding circadian proteins (6). And since known cell sigalling gases such as carbon monoxide (CO), nitric oxide (NO) and dioxygen ($O_2$) all bind to heme (and with different affinities), then the formation of a heme-bound PAS domain opens opportunities for the molecule to also respond to changes in concentrations of any or all of these cell signalling gases. Thinking in these terms, it may not be a coincidence that CO and NO production in cells is catalysed by two heme-containing proteins – heme oxygenase and nitric oxide synthase, respectively – both of which are themselves $O_2$-dependent. This interplay of heme- and gas-responsive PAS domains could provide the cell with highly versatile mechanisms for regulatory control, that are at the same time responsive to changing concentrations of heme, $O_2$, CO or NO. How these mechanisms play out has yet to be fully established.

In this paper, we present evidence from electrophysiological experiments for heme-dependent modulation of hERG3 (human *ether-à-go-go* related gene 3, alternatively known as Kv11.3). We identify an interaction of heme with a PAS domain contained within the channel. Our results provide insight on the role of heme in channel regulation; we use this to discuss how heme-induced structural changes might be used to control channel function .

## RESULTS

***Proteomics analyses.*** We sought to identify potential heme binding proteins in neuronal lysates from primary cortical neurons, using heme-affinity chromatography and mass spectrometry. Using this approach, we identified a number of proteins known to bind heme (*e.g.* mitochondrial enzymes) as well as proteins with unknown heme affinity; this included hERG3 (Fig. S1). In the structure of the overall hERG3 channel, there are four subunits each containing a transmembrane region as well as cytoplasmic N- and C-terminal regions, Fig. 1 (7). The N-terminal cytoplasmic region (approximately 400 residues) contains a highly conserved eag-domain (residues 1-135) which itself comprises a Cap domain (residues 1-25) and a Per-ARNT-Sim (PAS) domain (residues 26-135).

***Heme binding to the hERG3-eag domain***. We expressed the Cap domain (residues 1-26) and the PAS (27-135) domain of the hERG3 protein as an N-terminal $His_6$/S-tagged fusion protein in *E.coli* (Figs. 1 and S2); we will refer to this protein as hERG3-eag. On addition of heme to hERG3-eag, Fig. 2A, a species with Soret bands at 420 and 370 nm is observed, which we assign as arising from six- and five- coordinated heme, respectively. There is also a broad absorption envelope at 500-600 nm and a ligand-to-metal charge transfer band at 650 nm (Fig. 2A). These bands are similar to those reported for heme bound to proteins through Cys, Cys/His or Cys/X coordination (Table S1 (8)). The presence of two bands in the Soret region is indicative of heterogeneity, which may arise either from changes in axial ligands or from different orientations of the bound heme (8-10). The ligands to the heme in hERG3 were not identified. The affinity of ferric heme for hERG3-eag was determined by titration ($K_d$ = 7.02 ± 0.35 μM, Fig. 2A, inset top). Heme affinity can also be extracted from the first-order rate constant for transfer of heme to apo-myoglobin (which has a very high affinity for heme (11)); we measured this rate constant as $k_{off}$ = 0.03 $s^{-1}$ (Fig. 2A, inset bottom), which is several orders of magnitude higher than for the globins and more in the range observed for other regulatory heme proteins (12).

***Spectroscopic analysis of heme binding.*** Resonance Raman spectroscopy was used to provide more quantitative insight into the interaction of hERG3-eag with heme. In the high-frequency region, the spectrum of free heme displays the distinctive features of a ferric five-coordinate high-spin complex (5c-HS), with characteristic bands at 1372 ($\nu_4$), 1490 ($\nu_3$), and 1570 $cm^{-1}$ ($\nu_2$) (Fig. 2B(i)). The $\nu_{10}$ mode of the 5c-HS species is hidden by the vinyl stretching bands expected in the 1610- to 1640 $cm^{-1}$ region (1618 $cm^{-1}$ for the in-plane and 1628 $cm^{-1}$ for the out-of-plane vinyl group (13)). The ferric hERG3-eag-heme complex shows significant differences from free heme (Fig. 2B(ii)). All the modes described for ferric five-coordinate high-spin complex (5c-HS) are present for the hERG3-eag-heme complex. Additionally, we observe bands at 1502 ($\nu_3$), 1553 & 1585 $cm^{-1}$ ($\nu_2$), and 1640 $cm^{-1}$ ($\nu_{10}$). These modes indicate the presence of a six-coordinate low-spin complex (6c-LS) (Table S1) (14). These resonance Raman data are in agreement with the absorption spectra above, and demonstrate the formation of a six-coordinated heme species with a specific binding environment. EPR analyses support these conclusions, as the spectrum of the hERG3-eag-heme complex shows the formation of a low-spin heme complex (Fig. 2C). The spectrum is indicative of a mixture of species and was best simulated with two components (see Fig. 2C). The g-values for both

are in good agreement with those of other ferric heme proteins bearing cysteine coordinated opposite a neutral sixth ligand (8). A Cys/His ligation is favoured for both components as suggested by the placement in the Blumberg-Peisach diagram (Fig. 2C).

Carbon monoxide (CO) binds tightly ($K_d$ = 1.03 ± 0.37 μM, Fig. 3A) to the ferrous hERG3-eag-heme complex, and gives a species (Soret band at 420 nm; Q-bands at 540 and 569 nm) that is characteristic of a normal CO-bound heme species. An identical species (Soret band at 420 nm; Q-bands at 540 and 569 nm), is formed on reaction of apo-hERG3-eag domain with a pre-formed heme-CO complex, and with an affinity ($K_d$ = 10.55 ± 1.34 μM, data not shown) that is within reasonable range of the $K_d$ for binding of CO to the ferrous hERG3-eag complex ($K_d$ = 1.03 ± 0.37 μM) as above. These spectra for the hERG3-heme-CO complex formed by two different routes are significantly different from that of a free heme-CO complex ($\lambda_{max}$ = 407, 537 and 567 nm (12)), which indicates formation of a specific protein-heme-CO complex. The CO ligand is easily dissociated ($k_{off}$ = 0.03 $s^{-1}$) in the presence of nitric oxide (Soret band at 390 nm, Fig. 3C), which is characteristic of a five-coordinated NO-bound heme protein complex (15,16). These data indicate that the hERG3-eag-heme complex is competent for binding of biologically relevant gaseous ligands.

***Structure of the hERG3-eag domain.*** The purified hERG3-eag protein was crystallised in the apo-form, in a monomeric state. The structure of the PAS domain (residues 18-135) is shown in Fig. 4A. The hERG3-eag domain has a canonical PAS fold that comprises of five antiparallel β-sheets flanked by 3 α-helices, forming a hydrophobic cleft. This cleft is formed between the inner face of the β–sheet and the conformationally mobile F-helix. It is conserved in PAS domains known to bind ligands, including heme (3). The hERG3-eag structure contains a Cys39-Cys64 disulphide bond (Fig. 4A) situated 12 residues from the F-helix, and 13 residues from the Cap domain. The role of the disulphide bond is currently unknown and was not tested in this work, but it may impart a redox sensing functionality to the PAS domain (as previously suggested (17-20)).

The first 17 residues at the N-terminus are not seen in interpretable electron density in the crystal; furthermore, residues 18-23 are of weak density, indicating heterogenetity in this region (the N-terminal Cap). Mass spectrometry data (Fig. S2C) show there is a mixture of molecular weights with varying degrees of truncation at the N-terminus (Fig. S2D), and the observed density most likely reflects this mixture. As a significant proportion of the protein is unaccounted for in the model, this probably explains the relatively high R values for a structure at this resolution (see Table S2). Despite attempts to obtain a co-crystal structure of heme-bound hERG3-eag, extensive co-crystallisation and soaking experiments were unsuccessful. As we have noted previously (6), this does not mean that heme cannot bind to the protein, as the spectroscopic data clearly demonstrate that it does. It is more likely that the particular conformation selected for in the crystal structure is incompatible with heme binding, so that heme cannot bind to the protein during the crystallisation process. Structural flexibility of the protein that is linked to the heme binding event (see Discussion) might also affect whether heme co-crytallises with the protein.

***Effect of heme on hERG3 channels.*** To measure the functional response of hERG3 channels to heme, hERG3 was heterologously expressed in CHO cells. In whole-cell recordings, $K^+$ currents were elicited with the characteristic features of the hERG family (Fig. 5A), including slow voltage dependent activation and deactivation, rapid onset and recovery from inactivation and inhibition by astemizole (data not shown). Application of heme (Fig. 5B-E) caused a substantial inhibition of hERG3 current at all potentials (shown here after >3 mins). Mean (± SEM) heme inhibition of peak tail currents with a test potential to +40 mV was 63 ± 12 % ($p<0.05$, n = 3). Heme caused a small but significant negative shift in the voltage for half maximal activation of 6.7 % ($p<0.05$, n = 3) (Fig. 5E). The lipophilic properties of heme and its ability to interact with membrane phospholipids allows it to be transported across the plasma membrane via passive diffusion (21). To test if addition of intracellular heme also inhibited hERG3 channels, currents were recorded using the inside-out configuration of the patch clamp technique and heme was applied directly to the cytoplasmic side of excised membrane patches. As reported with many other ionic currents, upon excision a rapid decrease of hERG3 currents was observed in inside-out macropatches, consistent with loss of channel activity (run-down) upon removing the channels from the cellular environment. Addition of PIP2 (10 μM) to the perfusate ameliorated run-down and resulted in stable recording conditions (Fig. 5G, H). Subsequent application of heme (Fig. 5F-H) to the intracellular side of the membrane caused inhibition of hERG3 currents in a similar manner as extracellularly applied heme in whole cell recordings. The time courses of heme inhibition

were comparable, suggesting factors other than membrane diffusion of heme determine rates of hERG3 current inhbition. . These data demonstrate that heme inhibits hERG3 channel activity, thus connecting the heme binding event to modulation of channel function.

## DISCUSSION

The *ether-à-go-go* (EAG, Kv10-12) family of voltage gated $K^+$ channels are regulators of neuronal and cardiac cell action potential firing (excitability). In humans, the family comprises hEAG, hERG and hELK channels (22,23). In this work, we have identified heme-dependent regulation of hERG3 channel activity. Formation of a six-coordinated heme species is supported from resonance Raman data, as well as EPR and UV-visible spectra, and a heme-binding PAS domain within the eag-domain of the channel has been identified.

Recent cryo-EM structural models of rat EAG1 and hERG1 confirm that the four eag-domains are arranged around the periphery of the tetrameric intracellular assembly formed by the cNBHD and C-linkers (24,25). The function of this large intracellular complex is to modulate voltage dependent gating; profoundly influencing the time course and amplitudes of potassium currents during physiological processes such as action potentials. It sits underneath the transmembrane domains, with the C-linker connecting directly with the S6 activation gate. The PAS domain makes contacts predominantly with the CNBHD, whereas the Cap-domain extends towards the interface between the voltage sensor, C-linker and channel pore and thus is perfectly positioned to influence voltage and time dependent gating properties. Interestingly, functional studies reveal that deletion of the PAS and Cap domains has differential effects on the gating properties of hERG1 and hEAG1, suggesting that specific contacts with gating machinery of the two channels are different (26,27) In hEAG1 channels, the eag-domain is also required for calcium-calmodulin dependent inhibition of current (26). hERG3 gating is similar to hERG1 and it is likely that the eag domain has a similar role in both channels, which is to slow deactivation gating and enhance inactivation gating.

PAS domains, which are known to bind heme (4,5), have well established roles in regulating the function of the related hERG1 channel (7,28,29), but heme binding to this channel has not been established. Heme has been shown to potently modulate the activity of a range of other potassium ion channels such as Kv1.4, large conductance $Ca^{2+}$-activated K channels and ATP activated K channels (12,30-36). Our observation that heme binding reduces hERG3 activity furthers the notion that heme plays a deliberate modulatory role in these ion channel systems. As we noted in the introduction, the capacity for the heme group to also bind cell signalling gases (CO, NO, $O_2$ or even $H_2S$) vastly broadens the range of stimuli that these ion channels could potentially be modulated by.

It is worth noting that heme is important for neuronal survival (37), and so a role for heme in the regulation of the 'neuronal' channels hERG2 and hERG3 might reasonably be anticipated. At present, the biological basis for an interaction of heme with hERG3 is unknown, but a significant portion of brain damage caused during haemorrhagic stroke is believed to be due to the longer lasting, cytotoxic effects of heme (38). More generally, an abundance of heme after traumatic events such as stroke and ischemia could conceivably disrupt the regulatory balance of ion channels in the brain and has cytotoxic implications for the cells involved (39). Heme dependent inhibition of hERG3 would reduce repolarising $K^+$ currents, potentially increasing neuronal excitability and susceptibility to cell death. An abundance of heme after traumatic events thus has the capacity to disrupt the dynamic processes surrounding the regulation of ion channel function if they are sensitive to heme.

We did not identify the heme binding location in hERG3-eag. However, we have compared the structure of apo-hERG3-eag with those of other heme-binding PAS domain proteins (*Ec*DOS (40) and FixL (41)). Overlay of hERG3 with those of *Ec*DOS and FixL shows that, compared to the apo-hERG3 structure, there is a large movement of the F-helix in the heme-bound *Ec*DOS and FixL structures to accommodate binding of the heme group, Fig. 4B, C. It is feasible, therefore, that a similar mode of heme binding might occur in hERG3 if its F-helix is similarly flexible. Relevant in this context is the disulphide bond between Cys39 and Cys64, which is located 12 residues from the F-helix via a flexible loop. It has been proposed that disulphide bridges might serve as redox sensors in cells, by switching between thiol and disulphide structures (17-20). Loss of the Cys39-Cys64 disulphide could facilitate movement of the F-helix, allowing heme to bind to the protein. The ligands to the bound heme are not identified as yet but candidate residues are His70, His77, and Cys66 (Fig. 4A), which are in the vicinity of the proposed heme binding site based on the comparison with *Ec*DOS and FixL. Cys/His axial ligations would be consistent with

our spectroscopic data and with known ligations in other regulatory heme proteins (4,5).

Based on our structure, we identify one further possible mechanism of heme-dependent regulation. The N-terminal Cap domain (residues 1-26) in hERG3-eag is mostly unresolved in our structure. In hERG1 the Cap domain, which contains a flexibly-linked, but stable amphipathic helix, is already known to affect channel activity (27,42,43). So in addition to affecting the conformation of the F-helix (as above), it is possible that heme binding to the PAS domain in hERG3 could also affect the orientation of the adjacent and potentially highly mobile Cap domain (Fig. 1). This N-terminus is oriented towards the pore in the structure of the channel (25), and movements of the Cap domain might affect the conformations of the nearby cyclic nucleotide-binding homology domain, C-linker, voltage sensing domain, or pore forming domains as shown Fig. 6. Structural adjustments of this kind, in response to heme binding, would provide a mechanism for closure of the channel, due to the proximity of the N-terminal Cap domain to vital regulatory domains of channel gating (25). Relevant in this context is the observation that free heme affects channel function in the A-type potassium channels and, crucially, that the heme binds to the inactivation domain on the N-terminal region (30). We have no evidence for heme binding directly to the Cap domain in hERG3-eag, but changes in conformation of the N-terminal regions – induced either directly (by heme binding to N-termini), or indirectly (by heme binding to adjacent domains, such as PAS) – might plausibly provide a mechanism for ion channel regulation.

## EXPERIMENTAL PROCEDURES

*Chemicals and reagents.* All reagents were from Sigma-Aldrich (Dorset, England) unless otherwise stated. CO solutions were prepared by bubbling bath solution with CO gas. Iron protoporphyrin IX (hemin, Fig. S1A) was purchased from Sigma Aldrich. Aqueous stock solutions of heme for all spectroscopic and electrophysiological experiments were prepared by dissolving solid heme in 0.1 M NaOH; final concentrations were calculated spectrophotometrically ($\varepsilon_{385}$ = 58.4 $mM^{-1}cm^{-1}$ (44)) and diluted accordingly to 500 nM prior to use.

*Heme-agarose affinity purification and mass spectrometry of neuronal lysates.* Neuronal lysates were screened for possible heme-binding proteins using a modification of a previously published heme-agarose affinity (45). Binding of target proteins to heme-agarose was performed as previously (46), with modifications, Fig. S1B, that minimise pulling down proteins that bind to the heme-agarose resin non-specifically. Full details are given in the supplementary information. Using this approach, only proteins that were displaced from the agarose beads to bind specifically to the (heme) competitor (*i.e.* more likely to be *bona fide* heme binding proteins) were identified and subjected to proteomics analysis, Fig. S1C. Data are available via ProteomeXchange with identifier PXD019887.

*Expression and Purification of hERG3-eag domain.* The human KCNH7 clone (imaGenes Gmbh, Berlin) was used to obtain a sequence encoding residues 1-135 of the N-terminus of the human hERG3 channel, which comprises the Cap (residues 1-26) and PAS (27-135) domains (Figs. 1 and S2A). We refer to the fragment encoding residues 1-135 as hERG3-eag. The hERG3-eag domain was expressed as an N-terminal $His_6$/S-tagged fusion protein in *E.coli* BL21(DE3) cells using a pLEICS-93 (PROTEX facility, University of Leicester) expression vector. Cell cultures in LB media were grown at 37 °C containing ampicillin (0.1%) to an optical density ($OD_{600}$) of 0.6-0.7, at which point the temperature was reduced to 18 °C and isopropyl *β*-D-thiogalactoside (IPTG, 0.2 mM) added. After overnight incubation, cells were harvested, suspended in lysis buffer (50 mM phosphate/100 mM NaCl, pH 7.00, 10% glycerol, 0.1% Triton, 0.1 M $MgSO_4$, 1 complete ULTRA Tablet Mini EASYpack[Roche], 1 mg/ml lysozyme and 1mg/ml DNAase), lysed by sonication and centrifuged to remove cell debris. Cell lysates were loaded onto a 5 ml $Ni^{2+}$-NTA (Qiagen) affinity column equilibrated with 50 mM phosphate/100 mM NaCl, pH 7.00, 10% (vol/vol) glycerol and 15 mM imidazole. After washing with equilibration buffer the $His_6$/S-tagged proteins were eluted with 50 mM phosphate/100 mM NaCl, pH 7.0, 10% glycerol and 100 mM EDTA. The $His_6$/S-tag was cleaved with a His-tagged TEV-protease during overnight dialysis. The $His_6$/S-tag and His-tagged TEV protease were removed by reverse $Ni^{2+}$-NTA affinity column and proteins were purified to homogeneity with size exclusion chromatography (Superdex 200, GE Healthcare) using 50 mM phosphate/100 mM NaCl, pH 7.0, Fig. S2B. Protein concentrations were determined using a Bradford assay.

*Optical Absorption Spectroscopy.* Absorption spectra (25.0 °C) were obtained using a double beam spectrophotometer (Perkin Elmer Lambda 40) or a Kontron Uvikon UV-vis spectrometer. Ferric heme-bound hERG3-eag was obtained by addition of heme to hERG3-eag in 50 mM

HEPES, 50 mM NaCl, pH 7.5. The reduced protein was obtained by anaerobic addition of dithionite, and the ferrous-CO complex by gentle bubbling of CO through the reduced protein. Values of $K_d$ for binding of ligands (heme, CO) to hERG3 (3-5 mM) were obtained at 25.0 ºC in 50mM HEPES/50mM NaCl, pH 7.5 as described previously (12). Heme dissociation was measured by reacting the ferric heme-hERG3-eag complex (6.4 μM) with a 5.6-fold excess of apo-myoglobin (36 μM); the reaction was followed at 408 nm (50 mM HEPES/50 mM NaCl pH 7.5).

*Resonance Raman Spectroscopy.* Samples (50 μL, in 50 mM HEPES, 50 mM NaCl, pH 7.5) of ferric heme and its complexes were prepared in quartz EPR tubes and placed in a homemade spinning cell, at room temperature, to avoid local heating and to prevent photo-dissociation and degradation. Protein concentrations were in the range 90-120 μM, and sub-stoiochiometric concentrations of heme (to 0.8 equivalents) were added to the protein to ensure that no excess of heme was present. Raman excitation at 413.1 nm was achieved with a laser power <10 mW from an Innova 90 $Kr^+$ laser (Coherent, Palo Alto, California). Resonance Raman spectra were recorded using a two-stage monochromator (U1000, Jobin Yvon, Longjumeau, France) equipped with a front illuminated, deep-depleted CCD detector (Jobin Yvon, Longjumeau, France). Spectra correspond to an average of three different 1 h accumulations. The spectral accuracy was estimated to be ±1 $cm^{-1}$. Baseline correction was performed using GRAMS 32 (Galactic Industries, Salem, NH) and Origin®. Sample integrity was verified by following resonance Raman spectral evolution during the experiment.

*EPR spectroscopy.* EPR spectra were recorded on an Elexsys 500 X-band spectrometer (Bruker) equipped with a continuous-flow ESR 900 cryostat and an ITC504 temperature controller (Oxford Instruments, Abingdon, UK). Simulations were performed by using the Easyspin software package (47) and routines written in the Dorlet laboratory. Samples (100 μl, 100 μM total heme concentration, 4- to 5-fold excess protein) of the ferric heme complexes of hERG3-eag were prepared in 50 mM HEPES and 50 mM NaCl, pH 7.5, and transferred to quartz EPR tubes.

*Electrophysiology*. hERG3 currents were expressed in Chinese hamster ovary (CHO) cells and currents were recorded using either whole-cell or macropatch (inside-out or cell attached) configurations of the patch clamp technique. hERG3 currents were recorded with an Axopatch 200 voltage clamp amplifier, and digitized using a Digidata 1440A interface, and acquired and analysed using pClamp 10.3 software (Molecular Devices, Sunnyvale, CA, USA). For whole cell recordings the intracellular solution contained (in mM): 30 KOH, 110 KCl, 1.2 $MgCl_2$, 1 $CaCl_2$, 10 EGTA, 5 HEPES, 1 ATP, titrated to pH 7.2 with KOH. Cells were superfused with normal bath solution containing (mM): 135 NaCl, 10 KCl, 5 glucose, 2 $MgCl_2$, 2 $CaCl_2$ and 10 HEPES, titrated to pH 7.3 with NaOH. Macropatch currents were recorded in equimolar $K^+$ solutions. The bath solution contained (in mM): 40 KOH, 80 KCl, 10 $K_2SO_4$, 10 HEPES, 5 EGTA, 5 HEDTA and 10 Glucose, pH 7.2. Pipette solution contained (in mM): 140 KCl, 1 $MgCl_2$, 0.1 $CaCl_2$ and 10 HEPES, pH 7.4. To prevent rapid and complete current run-down 10 μM Phosphatidylinositol 4,5-bisphosphate (PIP2) was added to the bath solution in all excised inside-out macropatch recordings**.**

Aqueous stock solutions of ferric heme for electrophysiology experiments were prepared by dissolving heme in 0.1 M aqueous NaOH and mixing for 10 min, followed by centrifugation at 4,000 g for 10 min, and dilution as required. Final solutions contained 1 mM reduced glutathione. Aliquots of heme were made fresh daily. All experiments were conducted at room temperature (22 ± 1 °C). Data are presented as mean ± SEM of *n* experiments.

*Crystallisation and Data Collection.* A crystal of hERG3-eag (amino acids 1-135) was grown using sitting drop vapour diffusion at 295 K. The crystallisation drop was set up by mixing hERG3-eag (15 mg/ml, in 50 mM NaCl, 1 mM TCEP) in a 1:1 ratio with reservoir solution (0.1 M NaCl, 0.1 M HEPES pH=7.5, 1.6 M $(NH_4)_2SO_4$). A transparent crystal appeared after 4 weeks. The crystal was prepared for X-ray diffraction by brief immersion in the reservoir solution containing 25% glycerol for cryo-protection followed by flash vitrification in liquid nitrogen. X-ray diffraction data were collected at Diamond Light Source on I03 beam line. 3600 images of 0.05 degree were collected with an exposure time of 0.039 s/image using 0.976 Å radiation. The crystal belongs to the space group $P4_32_12$ with unit cell dimensions a = b = 32.78 Å, c = 200.68 Å, α = β = γ = 90° (Table S2). Data were processed and scaled with DIALS software from the CCP4 program suite (48). The structure was determined by molecular replacement in PHASER (49) using the hERG1 PAS domain [PDB 4HQA (50)] as the search model and refined with REFMAC5 (51). The model was refined to a resolution of 1.39 Å with $R_{work}$ and $R_{free}$ values of 18.2% and 23.4%, respectively, the final cycles of refinement

included extrapolated hydrogen atoms with anisotropic atomic displacement parameters (B) for all atoms. Data collection and refinement statistics are in Table S2 (PDB ID 6Y7Q) and the weighting scheme is given in Table S3.

Mass spectrometry analysis was carried out on a hERG3-eag crystal. The crystal was dissolved in 50 mM Hepes, 50 mM NaCl pH 7.5 and LC-MS was carried out using an RSLCnano HPLC system (Thermo Scientific) and an LTQ-Orbitrap-Velos mass spectrometer (Thermo Scientific). Samples were loaded at 0.1 mL/min onto a Vydac C8 5µm 250mm x 1mm I.D. reverse phase column (Grace Davison). The protein was desalted for 10 minutes in the loading buffer (0.1% formic acid) before elution using a 10 minute linear gradient from 3-96% B (80% acetonitrile / 0.1% formic acid). The output of the column was sprayed directly into the H-ESI2 electrospray ion source of the mass spectrometer maintained at 5kV. The FT analyser was set to acquire 10 microscans over the m/z range 800-2000 Da in positive ion mode. The maximum injection time for MS was 150 ms and the AGC target setting was $3e^6$. Protein charge-state distributions were deconvoluted using the Xtract function of the Xcalibur program (version 2.1.0.1139, Thermo Scientific).

**Data Availability.** Atomic coordinates and diffraction data have been deposited in the Protein Data Bank (accession code 6Y7Q). Proteomics data are available via ProteomeXchange with identifier PXD019887.

**Acknowledgements.** We thank the late Dr. Xiaowen Yang in the Protein Expression Laboratory (PROTEX-University of Leicester) for preparing the expression clones, and Dr. Fred Muskett for helpful discussions on the purification of hERG3-eag. We acknowledge Dr. Chris Millard, Chitra Seewooruthun and Kirsty Ford for help with the acquisition of crystallographic data and the Diamond Light Source staff at beam line I03 (BAG MX14692-18). This work benefited from the Biophysics Platform of I2BC, supported by iBiSA and by the French Infrastructure for Integrated Structural Biology (FRISBI) ANR-10-INBS-05.

**Conflict of interest.** The authors declare that they have no conflicts of interest with the contents of this article.

**Author contributions.** ER and JSM conceived and coordinated the project. All other authors designed experiments, performed research and analysed data. ER coordinated writing of the paper, with assistance from JSM and all authors.

## REFERENCES

1. Taylor, B. L., Zhulin, I.B. (1999) PAS domains: internal sensors of oxygen, redox potential, and light. *Microbiol. Mol. Rev.* **63**, 479-506
2. Henry, J. T., and Crosson, S. (2011) Ligand-binding PAS domains in a genomic, cellular, and structural context. *Annual review of microbiology* **65**, 261-286
3. Moglich, A., Ayers, R. A., and Moffat, K. (2009) Structure and signaling mechanism of Per-ARNT-Sim domains. *Structure* **17**, 1282-1294
4. Shimizu, T., Lengalova, A., Martinek, V., and Martinkova, M. (2019) Heme: emergent roles of heme in signal transduction, functional regulation and as catalytic centres. *Chem Soc Rev* **48**, 5624-5657
5. Shimizu, T., Huang, D., Yan, F., Stranava, M., Bartosova, M., Fojtikova, V., and Martinkova, M. (2015) Gaseous O2, NO, and CO in signal transduction: structure and function relationships of heme-based gas sensors and heme-redox sensors. *Chemical reviews* **115**, 6491-6533
6. Freeman, S. L., Kwon, H., Portolano, N., Parkin, G., Venkatraman Girija, U., Basran, J., Fielding, A. J., Fairall, L., Svistunenko, D. A., Moody, P. C. E., Schwabe, J. W. R., Kyriacou, C. P., and Raven, E. L. (2019) Heme binding to human CLOCK affects interactions with the E-box. *Proc Natl Acad Sci U S A* **116**, 19911-19916
7. Cabral, J. H. M., Lee, A., Cohen, S.L., Chait, B.T., Li, M., Mckinnon, R. (1998) Crystal Structure and Functional Analysis of the HERG Potassium Channel N Terminus: A Eukaryotic PAS Domain. *Cell* **95**, 649-655

8. Smith, A. T., Pazicni, S., Marvin, K. A., Stevens, D. J., Paulsen, K. M., and Burstyn, J. N. (2015) Functional divergence of heme-thiolate proteins: a classification based on spectroscopic attributes. *Chemical reviews* **115**, 2532-2558
9. Reynolds, M. F., Shelver, D., Kerby, R. L., Parks, R. B., Roberts, G. P., and Burstyn, J. N. (1998) EPR and electronic absorption spectroscopies of the CO-sensing CooA protein reveal a cysteine-ligated low-spin ferric heme. *Journal of the American Chemical Society* **120**, 9080-9081
10. Pazicni, S., Lukat-Rodgers, G. S., Oliveriusova, J., Rees, K. A., Parks, R. B., Clark, R. W., Rodgers, K. R., Kraus, J. P., and Burstyn, J. N. (2004) The redox behavior of the heme in cystathionine beta-synthase is sensitive to pH. *Biochemistry* **43**, 14684-14695
11. Hargrove, M. S., Singleton, E.W., Quillin, M.L., Ortiz, L.A., Jr., Olson, J.S. Mathews, A.J. (1982) His64(E7)-Tyr apomyoglobin as a reagent for measuring rates of hemin dissociation. *J. Biol. Chem.* **269**, 4207-4214
12. Kapetanaki, S. M., Burton, M. J., Basran, J., Uragami, C., Moody, P. C. E., Mitcheson, J. S., Schmid, R., Davies, N. W., Dorlet, P., Vos, M. H., Storey, N. M., and Raven, E. (2018) A mechanism for CO regulation of ion channels. *Nat Commun* **9**, 907
13. Kalsbeck, W. A., Robertson, D.E., Pandey, R.K., Smith, K.M., Dutton, P.L., Bocian, D.F. (1996) Structural and Electronic Properties of the Heme Cofactors in a Multi-Heme Synthetic Cytochrome. *Biochemistry* **35**, 3429-3438
14. Kitanishi, K., Igarashi, J., Hayasaka, K., Hikage, N., Saiful, I., Yamauchi, S., Uchida, T., Ishimori, K., and Shimizu, T. (2008) Heme-binding characteristics of the isolated PAS-A domain of mouse Per2, a transcriptional regulatory factor associated with circadian rhythms. *Biochemistry* **47**, 6157-6168
15. Stone, J. R., Sands, R. H., Dunham, W. R., and Marletta, M. A. (1995) Electron paramagnetic resonance spectral evidence for the formation of a pentacoordinate nitrosyl-heme complex on soluble guanylate cyclase. *Biochem Biophys Res Commun* **207**, 572-577
16. Stone, J. R., and Marletta, M. A. (1994) Soluble guanylate cyclase from bovine lung: activation with nitric oxide and carbon monoxide and spectral characterization of the ferrous and ferric states. *Biochemistry* **33**, 5636-5640
17. Gupta, N., and Ragsdale, S. W. (2011) Thiol-disulfide redox dependence of heme binding and heme ligand switching in nuclear hormone receptor rev-erb{beta}. *J Biol Chem* **286**, 4392-4403
18. Yi, L., Jenkins, P. M., Leichert, L. I., Jakob, U., Martens, J. R., and Ragsdale, S. W. (2009) Heme regulatory motifs in heme oxygenase-2 form a thiol/disulfide redox switch that responds to the cellular redox state. *J Biol Chem* **284**, 20556-20561
19. Yi, L., Morgan, J. T., and Ragsdale, S. W. (2010) Identification of a thiol/disulfide redox switch in the human BK channel that controls its affinity for heme and CO. *J Biol Chem* **285**, 20117-20127
20. Yi, L., and Ragsdale, S. W. (2007) Evidence that the heme regulatory motifs in heme oxygenase-2 serve as a thiol/disulfide redox switch regulating heme binding. *J Biol Chem* **282**, 21056-21067
21. Light, W. R., 3rd, and Olson, J. S. (1990) Transmembrane movement of heme. *J Biol Chem* **265**, 15623-15631
22. Asher, V., Sowter, H., Shaw, R., Bali, A., and Khan, R. (2010) Eag and HERG potassium channels as novel therapeutic targets in cancer. *World J Surg Oncol* **8**, 113
23. Ganetzky, B., Robertson, G. A., Wilson, G. F., Trudeau, M. C., and Titus, S. A. (1999) The eag family of K+ channels in Drosophila and mammals. *Annals of the New York Academy of Sciences* **868**, 356-369
24. Whicher, J. R., and MacKinnon, R. (2016) Structure of the voltage-gated K(+) channel Eag1 reveals an alternative voltage sensing mechanism. *Science* **353**, 664-669
25. Wang, W., and MacKinnon, R. (2017) Cryo-EM Structure of the Open Human Ether-a-go-go-Related K(+) Channel hERG. *Cell* **169**, 422-430 e410
26. Lorinczi, E., Helliwell, M., Finch, A., Stansfeld, P. J., Davies, N. W., Mahaut-Smith, M., Muskett, F. W., and Mitcheson, J. S. (2016) Calmodulin Regulates Human Ether a Go-Go 1 (hEAG1) Potassium Channels through Interactions of the Eag Domain with the Cyclic Nucleotide Binding Homology Domain. *J Biol Chem* **291**, 17907-17918
27. Muskett, F. W., Thouta, S., Thomson, S. J., Bowen, A., Stansfeld, P. J., and Mitcheson, J. S. (2011) Mechanistic insight into human ether-a-go-go-related gene (hERG) K+ channel

deactivation gating from the solution structure of the EAG domain. *J Biol Chem* **286**, 6184-6191
28. Chen, J., Zou, A., Splawski, I., Keating, M. T., and Sanguinetti, M. C. (1999) Long QT syndrome-associated mutations in the Per-Arnt-Sim (PAS) domain of HERG potassium channels accelerate channel deactivation. *J Biol Chem* **274**, 10113-10118
29. Gianulis, E. C., Liu, Q., and Trudeau, M. C. (2013) Direct interaction of eag domains and cyclic nucleotide-binding homology domains regulate deactivation gating in hERG channels. *J Gen Physiol* **142**, 351-366
30. Sahoo, N., Goradia, N., Ohlenschlager, O., Schonherr, R., Friedrich, M., Plass, W., Kappl, R., Hoshi, T., and Heinemann, S. H. (2013) Heme impairs the ball-and-chain inactivation of potassium channels. *Proc Natl Acad Sci U S A* **110**, E4036-4044
31. Tang, X. D., Xu, R., Reynolds, M. F., Garcia, M. L., Heinemann, S. H., and Hoshi, T. (2003) Haem can bind to and inhibit mammalian calcium-dependent Slo1 BK channels. *Nature* **425**, 531-535
32. Jaggar, J. H., Li, A., Parfenova, H., Liu, J., Umstot, E. S., Dopico, A. M., and Leffler, C. W. (2005) Heme is a carbon monoxide receptor for large-conductance Ca2+-activated K+ channels. *Circ Res* **97**, 805-812
33. Burton, M. J., Kapetanaki, S. M., Chernova, T., Jamieson, A. G., Dorlet, P., Santolini, J., Moody, P. C. E., Mitcheson, J. S., Davies, N. W., Schmid, R., Raven, E. L., and Storey, N. M. (2016) A heme-binding domain controls regulation of ATP-dependent potassium channels. *P Natl Acad Sci USA* **113**, 3785-3790
34. Augustynek, B., Kudin, A. P., Bednarczyk, P., Szewczyk, A., and Kunz, W. S. (2014) Hemin inhibits the large conductance potassium channel in brain mitochondria: a putative novel mechanism of neurodegeneration. *Experimental neurology* **257**, 70-75
35. Wang, S., Publicover, S., and Gu, Y. (2009) An oxygen-sensitive mechanism in regulation of epithelial sodium channel. *Proc Natl Acad Sci U S A* **106**, 2957-2962
36. Wu, J. Y., Qu, H. Y., Shang, Z. L., Tao, S. T., Xu, G. H., Wu, J., Wu, H. Q., and Zhang, S. L. (2011) Reciprocal regulation of Ca(2)+-activated outward K+ channels of Pyrus pyrifolia pollen by heme and carbon monoxide. *New Phytol* **189**, 1060-1068
37. Smith, A. G., Raven, E. L., and Chernova, T. (2011) The regulatory role of heme in neurons. *Metallomics : integrated biometal science* **3**, 955-962
38. Li, Z. (2011) *Heme Biology The Secret Life of Heme in Regulating Diverse Biological Processes* World Scientific
39. Robinson, S. R., Dang, T. N., Dringen, R., and Bishop, G. M. (2009) Hemin toxicity: a preventable source of brain damage following hemorrhagic stroke. *Redox Rep* **14**, 228-235
40. Kurokawa, H., Lee, D. S., Watanabe, M., Sagami, I., Mikami, B., Raman, C. S., and Shimizu, T. (2004) A redox-controlled molecular switch revealed by the crystal structure of a bacterial heme PAS sensor. *J Biol Chem* **279**, 20186-20193
41. Gong, W., Hao, B., and Chan, M. K. (2000) New mechanistic insights from structural studies of the oxygen-sensing domain of Bradyrhizobium japonicum FixL. *Biochemistry* **39**, 3955-3962
42. Ng, C. A., Hunter, M. J., Perry, M. D., Mobli, M., Ke, Y., Kuchel, P. W., King, G. F., Stock, D., and Vandenberg, J. I. (2011) The N-terminal tail of hERG contains an amphipathic alpha-helix that regulates channel deactivation. *PloS one* **6**, e16191
43. Wang, J., Myers, C. D., and Robertson, G. A. (2000) Dynamic control of deactivation gating by a soluble amino-terminal domain in HERG K(+) channels. *J Gen Physiol* **115**, 749-758
44. Dawson, R. M. C., Elliot, D. C., Elliot, W. H., and Jones, K. M. (1975) *Data for Biochemical Research*, Oxford University Press, Oxford, U.K
45. Otto, B. R., van Dooren, S. J., Nuijens, J. H., Luirink, J., and Oudega, B. (1998) Characterization of a hemoglobin protease secreted by the pathogenic Escherichia coli strain EB1. *The Journal of experimental medicine* **188**, 1091-1103
46. Lee, B. G. (1992) Isolation of an Outer Membrane Hemin-Binding Protein of *Haemophilus Influenzae* Type B. *Infection and Immunity* **60**, 810-816
47. Stoll, S., and Schweiger, A. (2006) EasySpin, a comprehensive software package for spectral simulation and analysis in EPR. *J Magn Reson* **178**, 42-55
48. Laboratory, S. D. (1994) The *CCP*4 suite: Programs for Protein Crystallography. *Acta Cryst. D* **50**, 760-763

49. McCoy, A. J., Grosse-Kunstleve, R. W., Adams, P. D., Winn, M. D., Storoni, L. C., and Read, R. J. (2007) Phaser crystallographic software. *Journal of applied crystallography* **40**, 658-674
50. Adaixo, R., Harley, C. A., Castro-Rodrigues, A. F., and Morais-Cabral, J. H. (2013) Structural properties of PAS domains from the KCNH potassium channels. *PloS one* **8**, e59265
51. Murshudov, G. N., Vagin, A.A., Dodson, E.J. (1997) Refinement of Macromolecular Structures by the Maximum-Likelihood Method. *Acta Cryst.* **53**, 240-255

## FOOTNOTES

This work was funded by Biotechnology and Biological Sciences Research Council Grants BB/K000128/1 and BB/M018598/1.

The abbreviations used are: PAS, (Per-ARNT-Sim) domain; hERG3-eag, residues 1-35 of the N-terminus of the human hERG3 channel, comprising the Cap and PAS domains; PIP2, phosphatidylinositol 4,5-bisphosphate.

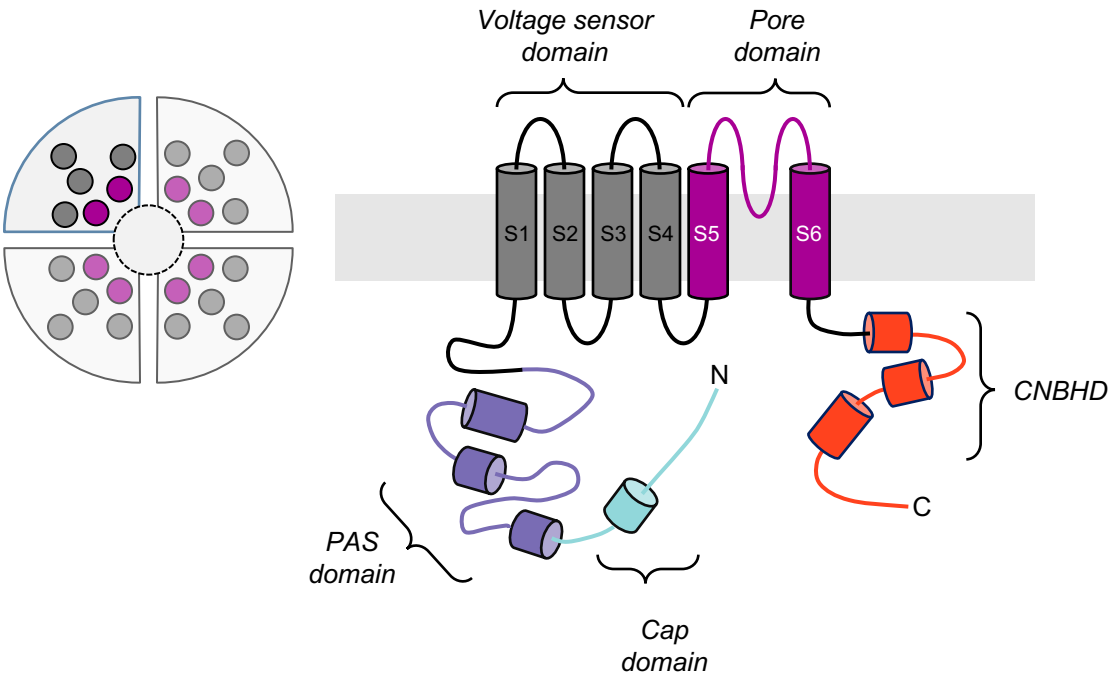


**Figure 1**. Schematic of the hERG3 channel subunit. hERG, which is part of the EAG family of ion channels, has four subunits which assemble to form a tetrameric structure (left). Each subunit contains a transmembrane region as well as cytoplasmic N- and C-terminal regions. The transmembrane region contains voltage sensor (helices S1-S4, dark grey) and pore-forming (helices S5-S6, magenta) domains inside the membrane bilayer. The C-terminal cytoplasmic region contains a cyclic nucleotide-binding homology domain (CNBHD, red), which is connected to the transmembrane region via a structured domain usually referred to as the C-linker. The N-terminal cytoplasmic region (approximately 400 residues) contains a region that is known as the eag domain (residues 1-135), which itself comprises a Cap domain (residues 1-25, light blue) and a PAS domain (residues 26-135, purple). This eag-domain fragment (residues 1-135) has been expressed in this work and is referred to as hERG3-eag in this paper.

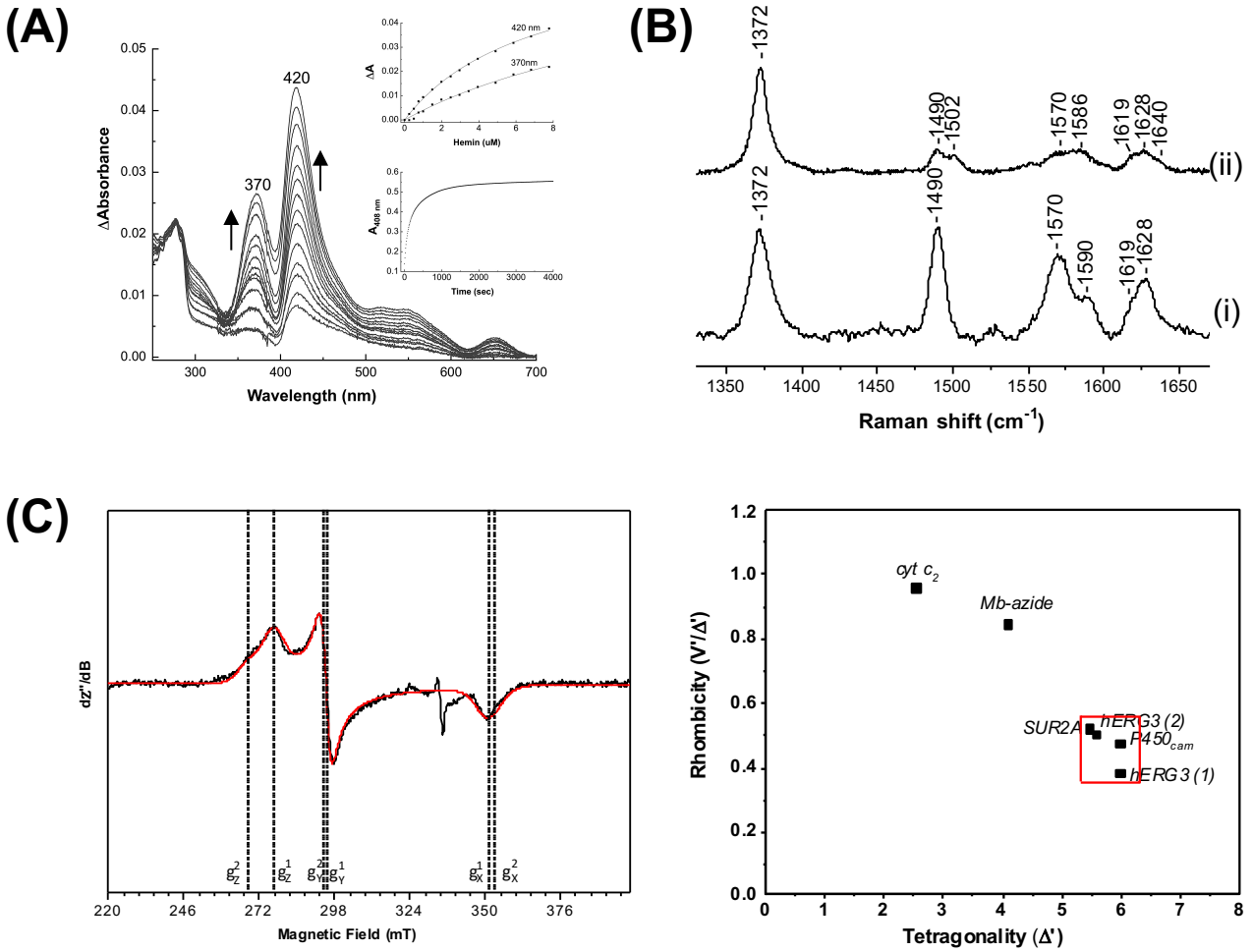


**Figure 2.** Analysis of heme binding to the hERG3-eag domain. **(A)** Difference spectra obtained on titration of the hERG3-eag domain with ferric heme; the arrows represent the directions of the absorbance changed with increasing heme concentration. Inset (top): Hyperbolic fitting of the heme binding data at both wavelength maxima to a 1:1 model for heme binding. Inset (bottom): Absorbance changes at 408 nm on binding of the ferric hERG3-eag complex to apo-myoglobin. Data were fitted to the first order decay process, yielding $k_{obs}$ = 0.03 $s^{-1}$. **(B)** Room temperature high-frequency resonance Raman spectra of (i) free heme, (ii) the ferric hERG3-eag-heme complex. All spectra were collected with 413.1 nm laser excitation. **(C)** Left: X-band EPR spectrum (black trace) of the ferric hERG3-eag-heme complex in the low-spin region along with the simulated spectrum (red trace). Experimental conditions: microwave frequency, 9.38 GHz; microwave power, 0.064 mW; field modulation amplitude, 2 mT; field modulation frequency, 100 kHz; temperature, 15 K; [heme] = 100 µM, 5-fold excess of protein in HEPES buffer 50 mM, pH 7.5, NaCl 50 mM. Simulation parameters : species 1 (75%) g-values (g-strain) $g_{z1}$ = 2.42 (0.06) $g_{y1}$ = 2.27 (0.00) $g_{x1}$ = 1.91 (0.04); species 2 (25%) g-values (g-strain) $g_{z2}$ = 2.50 (0,07) $g_{y2}$ = 2.28 (0.00) $g_{x2}$ = 1.90 (0.06); Lorentzian linewidth full-width at half-maximum 4mT. Right: Blumberg-Peisach correlation diagram showing EPR parameters plotted for various heme proteins.

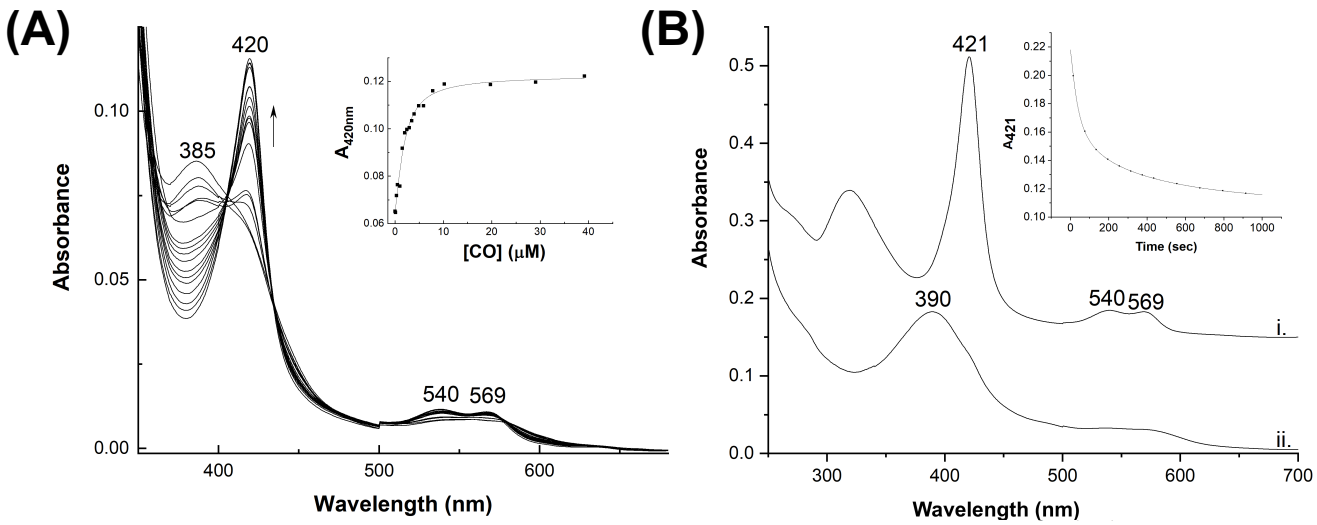


**Figure 3. (A)** Spectrophotometric titration of the ferrous hERG3-eag-heme complex with CO. Inset: quadratic (Morrison) fitting to the binding curve to give $K_d$ = 1.03 ± 0.37 μM. **(B)** Formation of a heme-NO-hERG3 complex ($\lambda_{max}$ = 390 nm) on dissociation of CO from the ferrous heme-hERG3 complex (3 μM, $\lambda_{max}$ = 421 nm) in the presence of NO. NO was formed from the NO releasing molecule, S-nitroso-N-acetyl penicillamine (see Methods). Inset: the 421 nm time course, fitted to a three-exponential process; using the dominant (50%) phase a rate constant for dissociation of CO, $k_{off(CO)}$, was determined ($k_{off(CO)}$ = 0.03 $s^{-1}$).

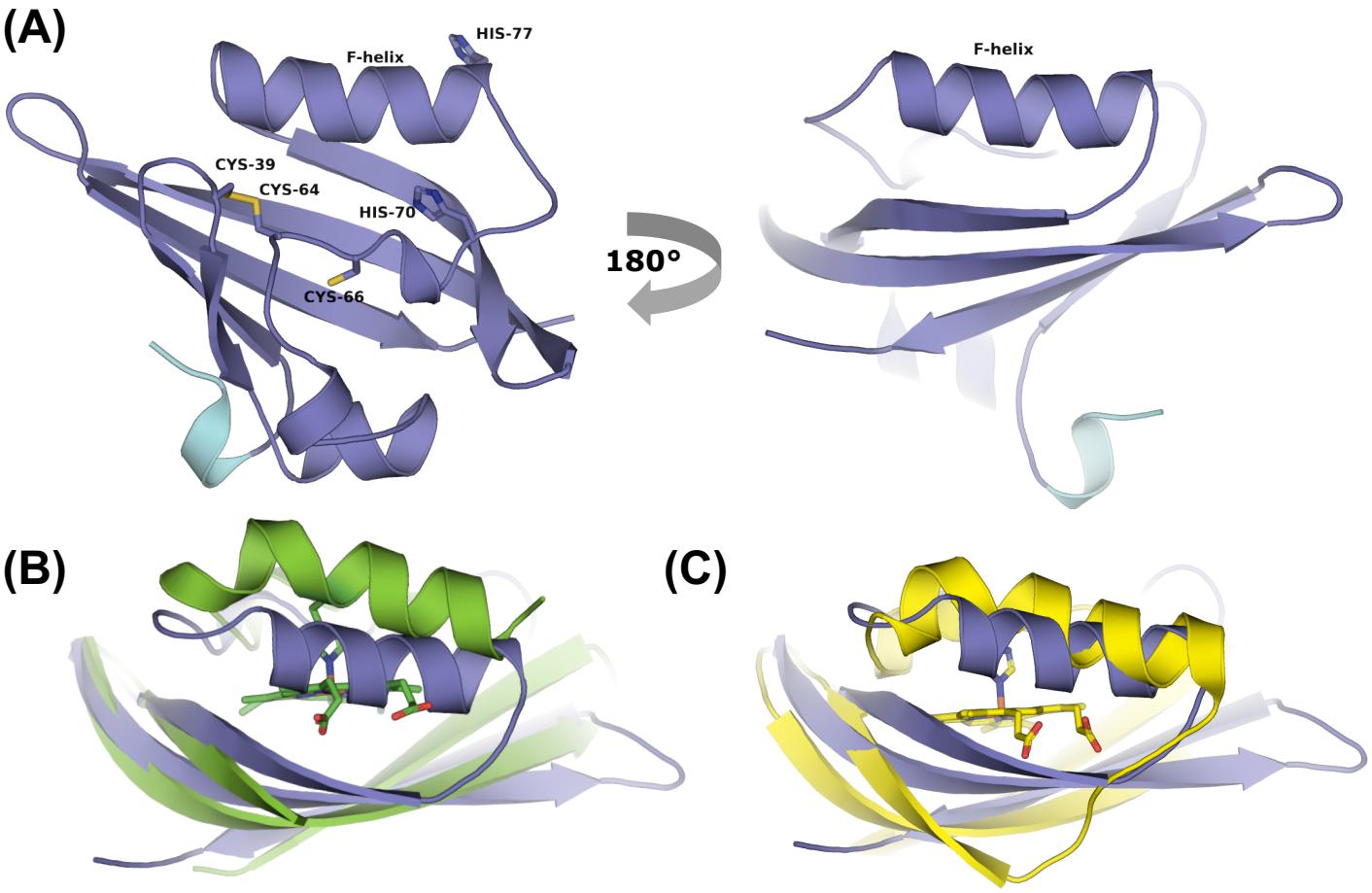


**Figure 4. (A)** Cartoon representation of the hERG3-eag crystal structure showing the PAS (purple) and Cap (light blue) domains; the colour scheme used is the same as that used in Fig. 1 for the PAS and Cap domains. Potential heme binding residues are labelled. **(B)** and **(C).** Structural alignment of hERG3-eag with structures of heme-bound PAS domains in *E. coli* DOS (1V9Y, green in (B)) and FixL (1DP6, yellow in (C)). Movement of the F-helix in *E. coli* DOS and FixL allows binding of the heme.

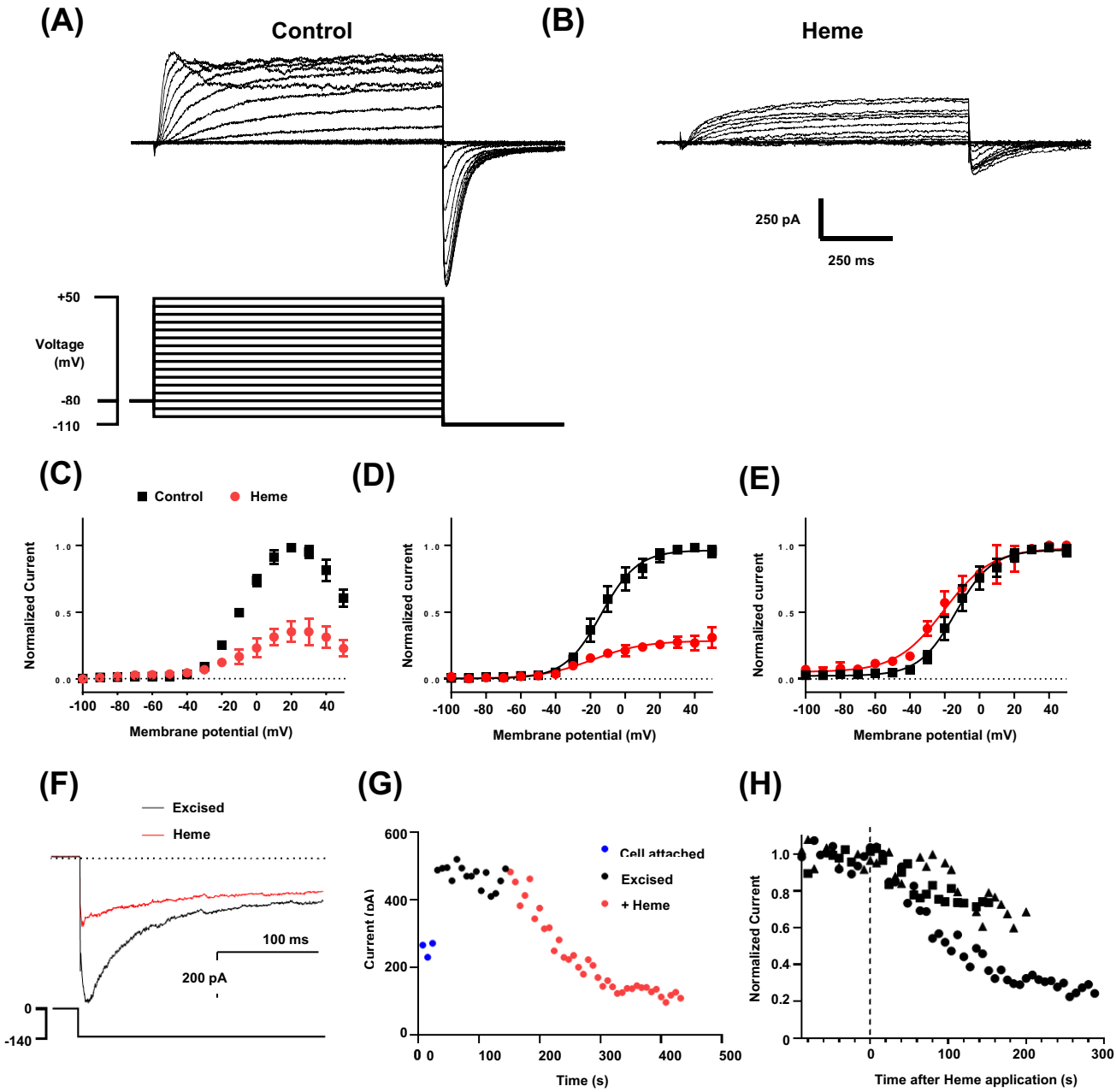


**Figure 5. hERG3 currents are inhibited by heme. (A)** Representative whole-cell hERG3 currents (upper panel) elicited with voltage protocol (lower panel) consisting of 1-s test pulses from -100 to +50 mV in 10 mV increments and from a holding potential of -80 mV. Inward tail currents were measured at a potential of -110 mV. The start-start interval for the voltage protocol was 5-s. **(B)** A family of hERG3 current traces from the same cell shown in (A) after superfusion of heme (500 nM). **(C)** Mean end-pulse current-voltage relationship with and without heme (500 nM) (n = 3). **(D, E)** Mean tail current (normalised to maximum control current in individual cells (D) or normalised to maximum current (E) in each recording solution) and plotted against test-pulse potential, with and without heme (500 nM) (n = 3). Data are fitted with Boltzmann functions (solid lines). Half maximal activation ($V_{0.5}$) and slope values were -12.3 ± 4.7 mV and 10.7 ± 1.0 mV respectively before heme and -19.0 ± 4.4 mV and 14.1 ± 2.6 mV with heme (n = 3). **(F)** Representative traces of excised inside-out macro-patch recordings of hERG3 tail currents before and during application of heme (1 µM). Patches were excised into solutions containing 10 µM phosphoinositol 4,5 bisphosphate to attenuate current run-down. Intracellular and extracellular solutions contained equimolar $K^+$ concentrations. Tail currents were measured at a potential of -140 mV and following 2-s test pulses to 0 mV (see voltage protocol in lower panel). Horizontal dotted lines indicate zero current (D-F). **G)** Representative plot of changes in amplitude of the deactivating component of the tail current plotted against time. The time between traces was 8-s. **(H)** Scatter plot of hERG3 tail current amplitudes in three separate excised patches plotted against time after heme application. Time of heme application is indicated by the vertical dashed line.

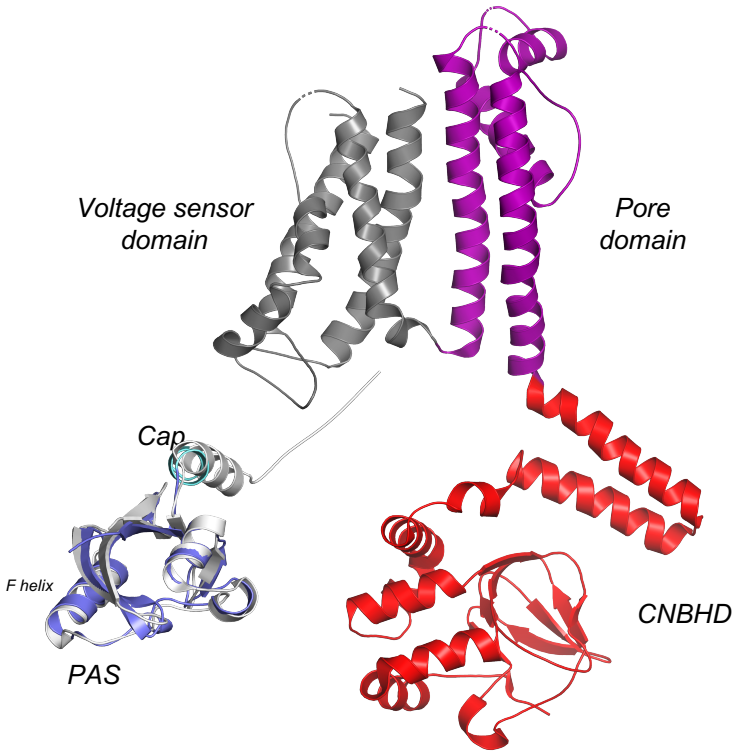


**Figure 6.** Cryo-EM structure of the hERG1 (Kv11.1) channel (5VA1), showing the cyclic nucleotide-binding homology domain (CNBHD, red), the pore domain (magenta), and the voltage sensing domain (dark grey). For direct comparison, the colour schemes used for the CNBHD, pore and voltage sensing domains are the same as those shown schematically in Fig. 1. In addition, the PAS and Cap (in light grey) domains are also shown for hERG1, aligned with hERG3-eag crystal structure (PAS domain, in purple; Cap domain in light blue, colour scheme as Fig. 1). Movements of the F-helix (labelled) or the Cap domain, induced by heme binding, might conceivably affect the conformations of the nearby CNBDH, pore, and voltage sensing domains which could provide a mechanism for channel regulation. Refer also to Fig. 1, which shows a schematic of the locations of each domain in relation to the overall channel structure. We have drawn cartoon schematics of heme-dependent regulation of several different ion channels previously ($K_{ATP}$, Slo1 (BK) and Kv1.4 channels (36)), and we envisage a similar mechanism of control here.